EDURA: an Evolvable Demonstrator for Upset Recovery Approaches with a 3D-printed Launcher

Torbjørn Cunis* and Murat Bronz†
French Civil Aviation School, 7 avenue Edouard Belin, Toulouse, France

Abstract

As in-flight loss of control has remained a severe threat to aviation, aeronautical research designed several approaches for upset recovery, few of which has been demonstrated in flight tests. The on-going success of micro air vehicles, however, rises the possibility of cheap and flexible flight demonstrations. In this paper, we present the concept of and first steps towards an aerial experimental platform for upset recovery: EDURA.

EDURA is part of the CONVEX project to investigate, develop, and demonstrate non-linear upset recovery control laws in a fixed-wing MAV.

1 Introduction

In-flight loss of control (LOC-I) imposes the *highest risk to aviation safety* [1] and has remained the foremost cause of fatal accidents for the last decades. Generally defined as any *deviation from the desired flight-path* by [2], LOC-I especially includes upset situations such as stall, high and inverted bank angle, as well as post-stall spirals and rotations [3]. With their unstable and highly non-linear characterizations, these situations require extensive control effort and adequate approaches to recover the upset aircraft and return into the flight envelope.

Non-linear behaviour of aircrafts in the post-stall flight regime has been investigated analytically [4–8] and in wind-tunnel studies [9, 10]. As a result, researchers developed control laws for upset recovery [11–20]. For the recovery approaches found in literature as well as proposed by the authors in [21] are model-based, there is a need for reliable flight dynamics data. However, though the NASA *generic transport model* (GTM) offers a scaled unmanned aerial platform, well-investigated in wind-tunnel studies, to test control systems [22], only Gregory et al. [20] report flight tests of the designed upset recovery approach.

In the past decade, the market for micro air vehicles (MAVs) has grown considerably. Widely available now, MAVs both offer cheap and repeatable experiments while being easy to replace and maintain in case of unsuccessful tests. On the other hand, indoor flight tests provide several benefits such as availability of accurate position tracking systems and reduction of disturbances in the test area, while requiring a small-scale vehicle other than the GTM.

Combining the mentioned points—accurate aerodynamic data, indoor tests, and usage of established MAV supply chains—, in this paper we are going to present concept and first version of a small-scale, fixed-wing experimental platform resembling an easy-to-model flying plate; based on a commercial-off-the-shell aircraft, for the first version, and the open-source autopilot software *Paparazzi UAV*. Furthermore, we will propose and present a catapult launcher allowing repeatable and configurable test conditions including those which actually pose an upset, like insufficient air speed, high angle of attack, or inverted bank angle. Based on a CAD model of the aircraft, we conclude with deriving its aerodynamic coefficients.

2 EDURA Concept

Indoor flight arenas, as existing at several research sites today, provide an ideal test environment for unmanned air vehicles. Wind and gust disturbances are reduced due to their closed walls and optical tracking systems provide position, attitude, and velocity information at both high accuracy and frequency. However, they are limited in space and hence unsuitable for larger vehicles. While clearly benefiting from indoor flight conditions, a suitable fixed-wing MAV is mainly required to be small.

Depron is a light-weight material which allows effortless processing. Wings cut of a single layer of depron show a rectangular surface and thus can be modelled as flying plate to obtain the aerodynamics coefficients. An aircraft made of depron offers design, making, and aerodynamic modelling of an aerial experimental platform in short iterations, evolving the flight dynamics as suitable. Furthermore, it accounts for the small-scale design necessary for indoor flight tests. Today's miniature microcontrollers, sensors and actuators, and auxiliary boards complete the setup albeit deliver full flight control and navigation on-board.

Eliminating the necessity of propulsion, a catapult launcher initially accelerates the aircraft to the desired air speed. In addition, it provides a configurable initial angle of attack and flight-path angle. The configuration of all three air speed, angle of attack, and flight-path angle after launch is repeatable over multiple executions of a single test case.

*Doctoral researcher at ENAC and ONERA – The French Aerospace Lab; torbjoern.cunis@recherche.enac.fr
†Assistant professor at ENAC; murat.bronz@enac.fr

(a) Side view.

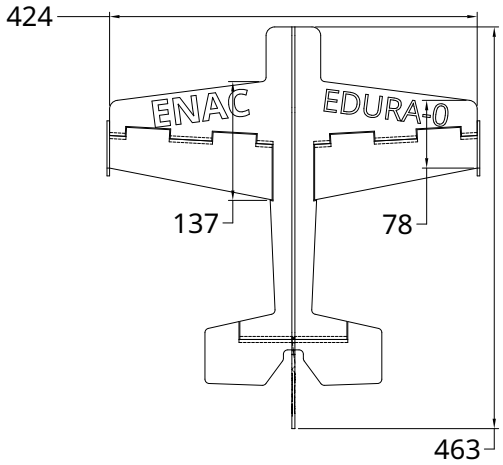

(b) Top view.

Figure 1: Side view (a) of the EDURA-0 vehicle based on an *E-flite UMX Yak 54 3D* commercial-off-the-shell aircraft; and CAD drawing (b) from the top with measures: wing span, root chord, tip chord, and length (Quantities in millimetres).

3 EDURA-0 Aircraft

The first aircraft is based on an *E-flite UMX Yak 54 3D* commercial off-the-shelf radio-controlled aircraft,[1] as shown in Fig. 1a. This 35 g vehicle with a wing span of 42.4 cm and length of 46.3 cm is made of 35 mm thick depron and resembles a flying plate with trapeze-shaped wings (Fig. 1b). The control surfaces, elevator, rudder, and left and right ailerons are driven by four linear servos at a speed of 0.14 s [23].

The E-flite aircraft has been originally shipped with a *Spectrum* radio receiver, which was replaced by a *Lisa-MXs* autopilot board [24] and an *ESP8266-9* wifi module for UDP-based communication (Fig. 2). The autopilot runs the open-source software *Paparazzi UAV*.[2]

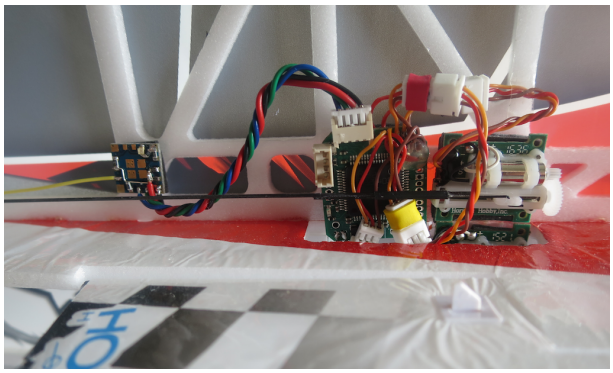

Figure 2: Autopilot configuration (from left to right): ESP8266-9 wifi module, Lisa-MXs board, and the linear servo for the elevator.

For unpropelled flight, the propellor and its motor will be removed and replaced by a respective weight for balance.

[1] http://www.e-fliterc.com/Products/?ProdID=EFLU3550
[2] http://paparazziuav.org

4 Catapult Launcher

There are three main requirements to a catapult launcher for upset recovery tests, as aforementioned: to accelerate the aircraft to a certain air speed; to establish the initial angle of attack; and define the flight-path, *i.e.* the flight-path angle and heading.

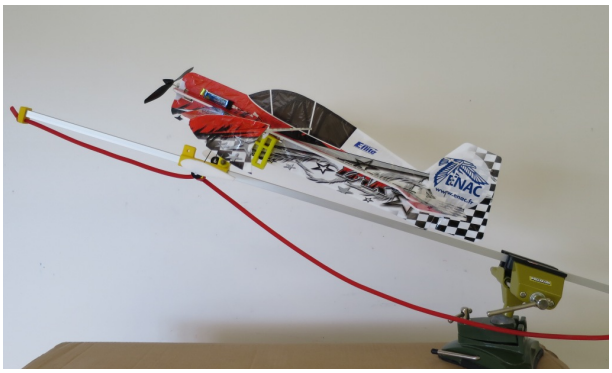

Figure 3: The EDURA catapult launcher with aircraft.

As for those, the catapult launcher is designed of three components (Figs. 3 and 4), the rail, a cart moving lateral along the rail, and a cage to carry the aircraft. The cart is accelerated by an elastic band fixed to the front of the rail, while the same band attached to the end, too, slows down the cart after ejecting the aircraft.

Rail The rail of the catapult launcher is based on a 1 m aluminium tube with quadratic surface and inner and outer edges of 8 mm and 10 mm, respectively. Front and back end stop-

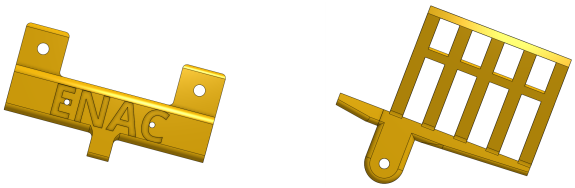

(a) Cart. (b) Cage.

Figure 4: Components of the catapult launcher in CAD.

pers were 3D-printed to attach the elastic band to as well as to prevent the cart from racing beyond the rail's ends. The orientation of the rail with respect to the global reference frame will define the flight-path vector of the aircraft.

Cart The cart has been designed in CAD (Appendix, Fig. 6) and was 3D-printed afterwards. Its quadratic body fits around the rail and allows lateral motion of one degree of freedom. The legs at the back of the cart allows the cage to be attached with a variable angle, defining the angle of attack. At the bottom, an eye is provided for the elastic band.

Cage Just as the cart, the cage was 3D-printed. Attached on top of the cart, it holds the aircraft during the acceleration and allows a smooth ejection. A CAD drawing of the cage is shown in the appendix (Fig. 7).

The initial air-speed, *i.e.* the speed of the cart with respect to the rail can be configured by pulling the cart backwards thus stretching the elastic to a certain length with respect to its resting point.

5 Aerodynamic Coefficients

Fuselage, wings, and control surfaces of the UMX Yak 54 3D aircraft were measured and modelled in CAD (Fig. 5a). Aerodynamic coefficients are obtained numerically by using a program based on vortex-lattice method, called AVL[3] (Fig. 5b). As a result, the linearized stability derivatives around the selected operating point are given in Tab. 1 for 4 m/s cruise speed and 15 % static margin. Based on the initial numerical estimation of the coefficients, a comparison can be made between the expected and measured flight trajectories. According to the comparison, it will be possible to verify the linear coefficients and identify the non-linear part in order to extend and improve the numerical estimation of the coefficients. An improved model, however, is crucial for the development of upset recovery approaches.

6 Conclusion

In this paper, we have argued the need of an experimental platform for flight tests of upset recovery approaches. We have therefore discussed the benefits of indoor flights of suitable MAVs and proposed the EDURA concept of an evolvable

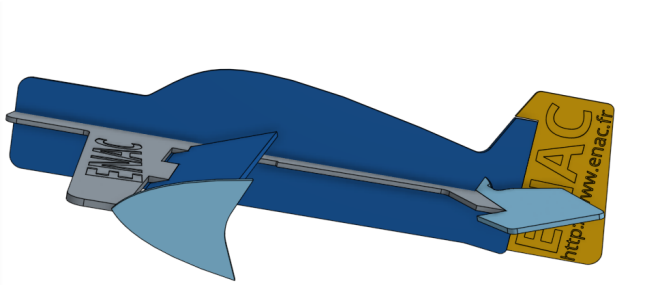

(a) CAD model.

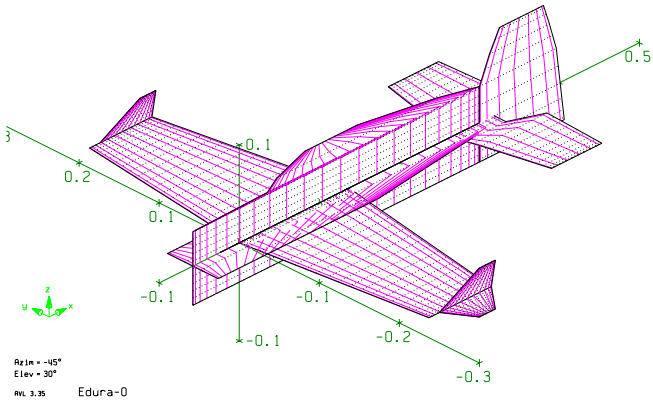

(b) AVL mesh.

Figure 5: CAD model of the EDURA-0 aircraft and its control surfaces (a) and AVL Mesh (b).

small-scale, fixed-wing MAV as demonstrator. An additional catapult launcher allows repetition of the initial flight conditions. The first prototype based on a commercial-off-the-shelf aircraft has as well been presented as the design and development of the catapult launcher.

The system illustrated is to be evaluated in launch tests with indoor position tracking in order to proof repeatability of the initial conditions. By free-flight force estimation and force measurement in wind-tunnel tests, future studies would verify the aerodynamic coefficients derived on the aircraft model. Overall, we have introduced an aerial experimental platform to test and demonstrate upset recovery approaches based on the aerodynamic model of the aircraft, where the *modus operandi* is going to allow the evolution of the vehicle's parameters and test conditions.

Acknowledgements

The authors wish to thank the TU Delft Micro Air Vehicle Laboratory for providing the Lisa-MXs hardware and support.

CAD models of aircraft and aircraft launcher were created in the free-to-use cloud platform *Onshape*.[4]

[3] `http://raphael.mit.edu/avl`

[4] `http://onshape.com`

	α	β	p	q	r	δ_{elv}	δ_{ail}	δ_{rud}
C_L	4.4478	0.0	0.0	8.2844	0.0	0.01506	0.0	0.0
C_Y	0.0	-0.7016	0.25792	0.0	0.82037	0.0	0.000254	0.0081
$C_{D_{ff}}$	-	-	-	-	-	0.001086	0.0	0.0
e	-	-	-	-	-	0.000486	0.0	0.0
C_l	0.0	-0.07259	-0.4150	0.0	0.09355	0.0	-0.008842.	0.0002
C_m	-0.6156	0.0	0.0	-10.133	0.0	-0.03268	0.0	0.0
C_n	0.0	0.14285	-0.09723	0.0	-0.44895	0.0	-0.000924	-0.00538

Table 1: Stability derivatives extracted from AVL program for the aircraft at 5 m/s equilibrium cruise speed. All derivatives are in 1/rad or s/rad except for the control derivatives δ, which are in $1/^\circ$.

References

[1] Unstable Approaches: Risk Mitigation Policies, Procedures and Best Practices. Technical report, International Air Transport Association, Montreal, CA, 2015.

[2] Airplane Flying Handbook. FAA handbook FAA-H-8083-3B, Flight Standards Service, Washington, US-DC, 2016.

[3] J. R. Chambers and S. B. Grafton. Aerodynamic Characteristics of Airplanes at High Angles of Attack. NASA technical memorandum NASA/TM-74097, Langley Research Center, Hampton, US-VA, 1977.

[4] James V Caroll and Raman K Mehra. Bifurcation Analysis of Nonlinear Aircraft Dynamics. *Journal of Guidance, Control, and Dynamics*, 5(5):529–536, 1982.

[5] Craig C Jahnke. *Application of Dynamical Systems Theory to Nonlinear Aircraft Dynamics*. Phd thesis, California Institute of Technology, Pasadena, US-CA, 1990.

[6] M.G. Goman, G.I. Zagainov, and A.V. Khramtsovsky. Application of bifurcation methods to nonlinear flight dynamics problems. *Progress in Aerospace Sciences*, 33(9–10):539–586, 1997.

[7] Harry G Kwatny, Jean-Etienne T Dongmo, Bor-chin Chang, Gaurav Bajpai, Murat Yasar, and Christine Belcastro. Nonlinear Analysis of Aircraft Loss of Control. *Journal of Guidance, Control, and Dynamics*, 36(1): 149–162, 2013.

[8] Jacobus Adriaan Albertus Engelbrecht, Simon J. Pauck, and Iain K. Peddle. A Multi-mode Upset Recovery Flight Control System for Large Transport Aircraft. In *AIAA Guidance, Navigation, and Control Conference*, Boston, US-MA, aug 2013.

[9] John V Foster, Kevin Cunningham, Charles M Fremaux, Gautam H Shah, and Eric C Stewart. Dynamics Modeling and Simulation of Large Transport Airplanes in Upset Conditions. In *AIAA Guidance, Navigation, and Control Conference and Exhibit*, San Francisco, US-CA, aug 2005.

[10] Neal T Frink, Patrick C Murphy, Harold L Atkins, Sally A Viken, Justin L Petrilli, Ashok Gopalarathnam, and Ryan C Paul. Computational Aerodynamic Modeling Tools for Aircraft Loss of Control. *Journal of Guidance, Control, and Dynamics*, 0(0), 2016.

[11] Frank W Burcham Jr, John J Burken, Trindel A Maine, and C Gordon Fullerton. Development and Flight Test of an Emergency Flight Control System Using Only Engine Thrust on an MD-11 Transport Airplane. NASA technical publication NASA/TP-97-206217, Dryden Flight Research Center, Edwards, US-CA, 1997.

[12] Frank W Burcham Jr, Richard Stevens, Ronald Broderick, and Kerry Wilson. Manual Throttles-Only Control Effectiveness for Emergency Flight Control of Transport Aircraft. In *9th AIAA Aviation Technology, Integration, and Operations Conference*, Hilton Head Island, US-SC, sep 2009.

[13] James M Urnes Sr. Flight Control for Multi-engine UAV Aircraft using Propulsion Control. In *AIAA Infotech@Aerospace*, Garden Grove, US-CA, 2012.

[14] Bor-Chin Chang, Harry G. Kwatny, Elie R. Ballouz, and David C. Hartmann. Aircraft Trim Recovery from Highly Nonlinear Upset Conditions. In *AIAA Guidance, Navigation, and Control Conference*, San Diego, US-CA, 2016.

[15] Enric Xargay, Naira Hovakimyan, and Chengyu Cao. $\mathcal{L}_1$ adaptive controller for multi-input multi-output systems in the presence of nonlinear unmatched uncertainties. In *IEEE American Control Conference*, pages 874–879, Baltimore, US-MD, 2010.

[16] Vahram Stepanyan, Kalmanje Krishnakumar, John Kaneshige, and Diana Acosta. Stall Recovery Guidance Algorithms Based on Constrained Control Approaches. In *AIAA Guidance, Navigation, and Control Conference*, San Diego, US-CA, 2016.

[17] Jacobus Adriaan Albertus Engelbrecht. *Automatic Flight Envelope Recovery for Large Transport Aircraft*.

Phd thesis, University of Stellenbosch, Matieland, ZA, 2016.

[18] Luis G Crespo, Sean P Kenny, David E Cox, and Daniel G Murri. Analysis of Control Strategies for Aircraft Flight Upset Recovery. In *AIAA Guidance, Navigation, and Control Conference*, Minneapolis, US-MN, aug 2012.

[19] Nathan D Richards, Neha Gandhi, Alec J Bateman, David H Klyde, and Amanda K Lampton. Vehicle Upset Detection and Recovery for Onboard Guidance and Control. *Journal of Guidance, Control, and Dynamics*, 0(0), 2016.

[20] Irene Gregory, Enric Xargay, Chengyu Cao, and Naira Hovakimyan. Flight Test of $\mathcal{L}_1$ Adaptive Control Law: Offset Landings and Large Flight Envelope Modeling Work. In *AIAA Guidance, Navigation, and Control Conference*, Portland, US-OR, aug 2011.

[21] Torbjørn Cunis, Laurent Burlion, and Jean-Philippe Condomines. Non-linear Analysis and Control Proposal for In-flight Loss-of-control. In *20th IFAC World Congress*, Toulouse, FR, 2017.

[22] Thomas L Jordan, John V Foster, Roger M Bailey, and Christine M Belcastro. AirSTAR: A UAV Platform for Flight Dynamics and Control System Testing. In *AIAA Aerodynamics Measurement Technology and Ground Testing Conference*, San Francisco, US-CA, 2006.

[23] Spektrum AR6410/AR6410L User Guide. Technical report, Horizon Hobby, Inc., 2012.

[24] Kimberly McGuire, Guido de Croon, Christophe De Wagter, Karl Tuyls, and Hilbert Kappen. Efficient Optical flow and Stereo Vision for Velocity Estimation and Obstacle Avoidance on an Autonomous Pocket Drone. *IEEE Robotics and Automation Letters*, 2(2): 1070–1076, 2017.

Appendix A: CAD Drawings

CAD drawings of the cart and cage components of the catapult launcher are shown in Figs. 6 and 7, respectively.

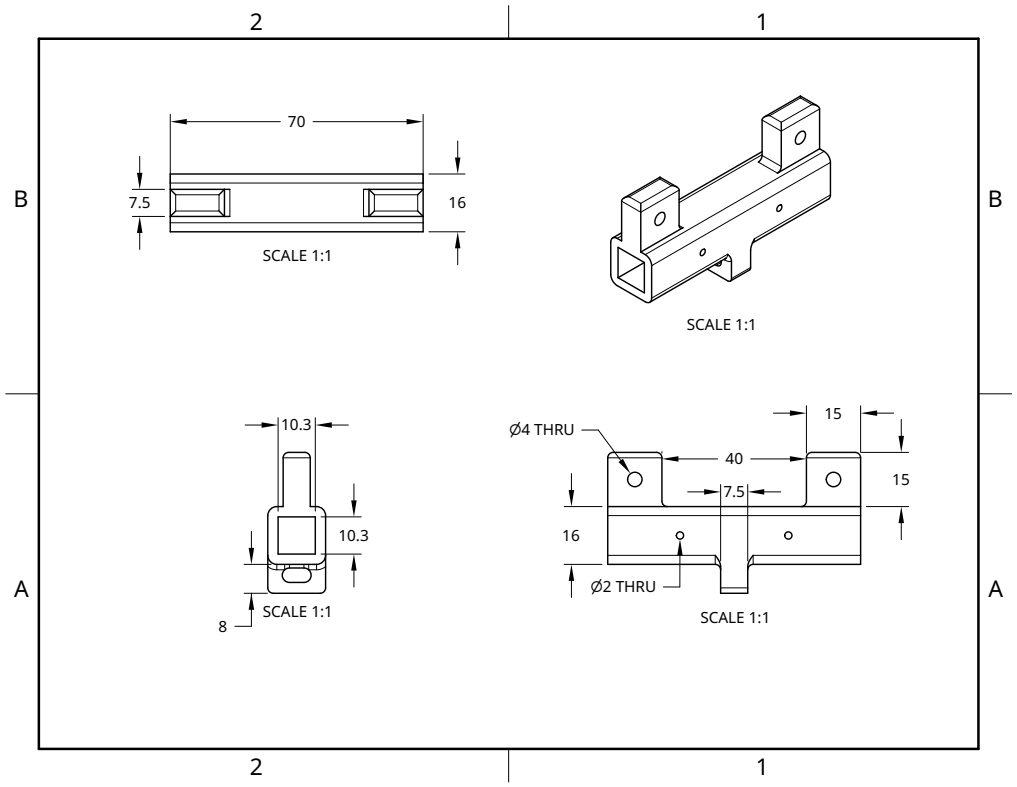

Figure 6: CAD drawing of the cart component of the catapult launcher. All quantities are given in millimetres.

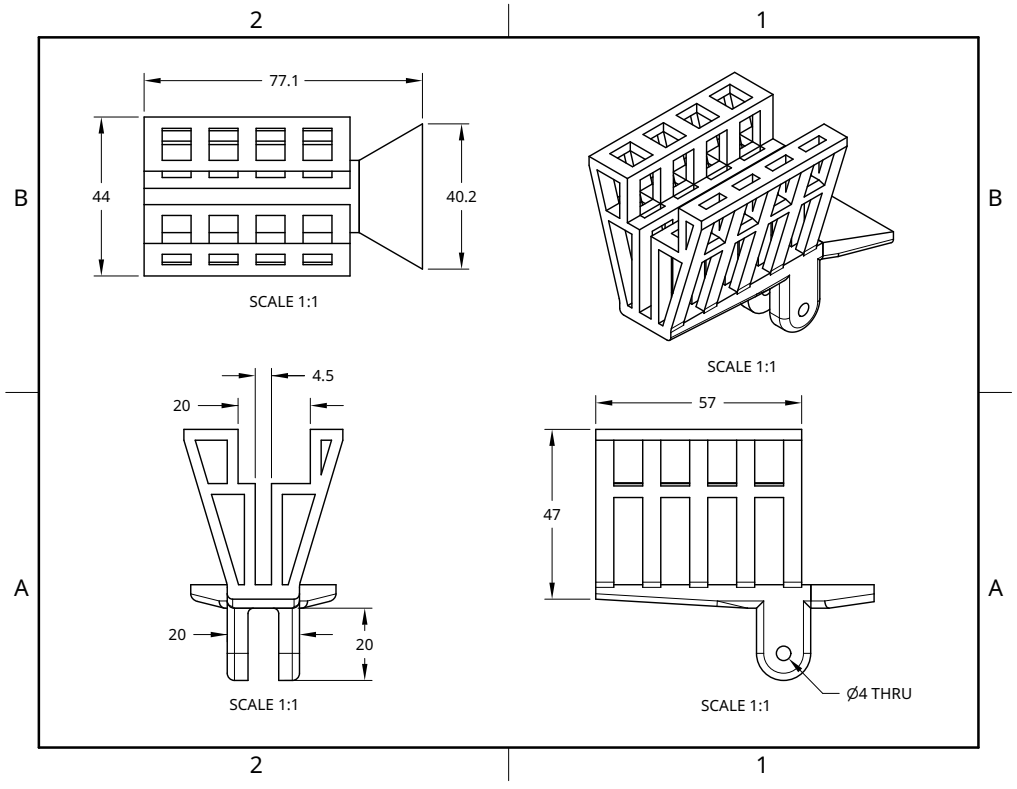

Figure 7: CAD drawing of the cage component of the catapult launcher. All quantities are given in millimetres.